Bioinspired Effective Prevention of Restacking in Multilayered Graphene Films: Towards the Next Generation of High-Performance Supercapacitors

*Xiaowei Yang, Junwu Zhu, Ling Qiu, and Dan Li**

A combination of extraordinary electrical, thermal, and mechanical properties makes graphene sheets not only attractive as atom-thick components in nanoelectronic devices, but also excellent molecular building blocks for assembling new macroscopic materials for widespread applications,[1] particularly as electrodes for energy storage devices.[1d,2] Since significant advances have recently been achieved in the cost-effective production of graphene in large amounts,[1b–e,3] large-scale application of graphene in a bulk assembly form appears to be close to the market.[1d] However, the exploitation of graphene-based bulk materials faces a key scientific and technical challenge. As with other polymeric or molecular materials, the performance of graphene-based materials is strongly affected by the way the individual sheets are arranged. Due to the intersheet van der Waals attractions, aggregation or restacking inevitably occurs in graphene assemblies.[2a,3a,4] Consequently, many of the unique properties that individual sheets possess, such as high specific surface area and peculiar electron transport behaviors, are significantly compromised or even unavailable in an assembly. For example, when used as electrodes for electrochemical capacitors or supercapacitors, physically separated graphene sheets that are vertically grown on a metal substrate show an exceptional frequency response.[5] This result, however, has been considered difficult to realize in porous bulk graphene films due to the increased difficulty of ions diffusion caused by intersheet aggregation.[5] The performance of bulk graphene films[2a–j] has yet to be significantly improved to compete with traditional porous carbon materials for large-scale use in energy storage devices.[6] Note that graphite is an assembly of graphene but lacks many of the attractive attributes of individual sheets as a consequence of dense packing. Effective prevention of intersheet restacking is essential to allow the individual sheets in multilayered graphene structures to behave as graphene rather than graphite.

We recently discovered that graphene prepared by chemical conversion from graphite can form stable aqueous colloids without the need for any surfactants.[7] This success has enabled us to manipulate the assembly of graphene using the principles of colloidal chemistry. In this work, we demonstrate that water, the very "soft" matter, can serve as an effective "spacer" to prevent the restacking of chemically converted graphene (CCG) sheets. In contrast to the common expectation that graphene sheets would restack to graphite when stacked face-to-face, hydrated CCG sheets can remain significantly separated when combined together in a nearly parallel manner (see schematic in **Figure 1**c). The high specific surface area of CCG sheets can be effectively harnessed in a readily available, macroscopically usable film form and it is thus ready to be integrated into various devices. The resultant self-stacked, solvated graphene (SSG) film exhibits unprecedented electrochemical performance, making it possible to make a new generation of supercapacitors that can combine high energy density, high power density, and high operation rates.

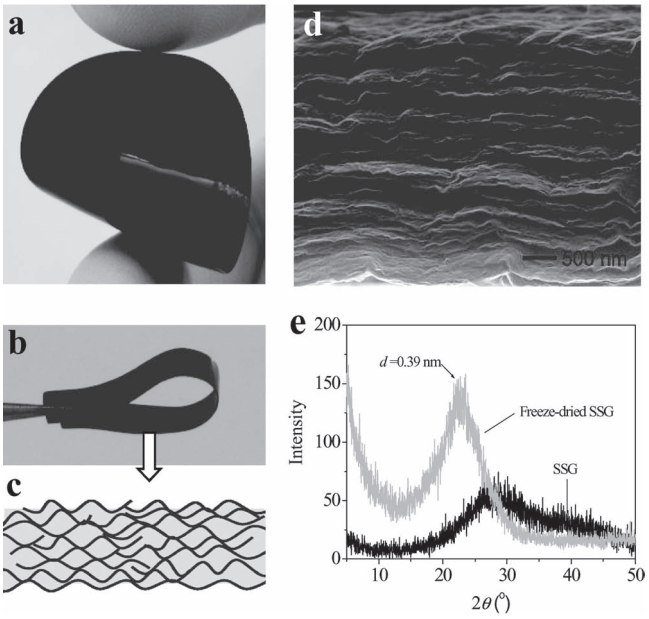

Figure 1. Structure of the SSG film. a,b) Photographs of the as-formed flexible SSG films. c) Schematic of the cross-section of the SSG film. d) SEM image of the cross-section of a freeze-dried SSG film. Given that the undried SSG film is approximately 20 times thicker than the dried one, the undried SSG film must be much more porous than shown in this SEM image. e) XRD patterns of as-prepared and freeze-dried SSG films. The broad diffraction peak of the wet SSG film (from 27.9° to 44.8°) is likely due to the water confined in the CCG network because the corresponding *d*-spacing is less than the $d_{(002)}$ of graphite. Further experiments are required to understand the structure of the water in this SSG film.

X. Yang, Dr. J. Zhu, L. Qiu, Prof. D. Li
Department of Materials Engineering
ARC Centre of Excellence for Electromaterials Science
Monash University
VIC 3800, Australia
E-mail: dan.li2@monash.edu

DOI: 10.1002/adma.201100261

Our concept was inspired by the fact that all biological tissues are more or less hydrated. In contrast, most of man-made functional materials and devices including graphene are used or supplied routinely in a dried, "hard" form even if their ultimate uses involve the contact with a liquid such as in supercapacitors.[2a–j] One of the important functions of hydration in biology lies in the fact that hydration can provide strong repulsive forces[8] to prevent cells and tissues from collapse and to enable the formation of interconnected water passages on different length scales to make each tissue function properly. If dried, the water passages in tissues are damaged, often in an irreversible manner. To be viable, biological tissues need to remain in a proper hydrated state since birth. These facts inspired us to look again at the strategies previously used for making graphene-based paper by vacuum filtration.[7]

As a simple and efficient technique for making macroscopic assemblies from a suspension of solid particles, filtration has been widely used for manufacturing writing paper since ancient times. Since the formation of graphene oxide paper by filtration was first reported by Ruoff and co-workers,[3] this technique has recently been adopted for fabricating graphene papers.[9] Nevertheless, only dried paper products have to date been targeted.[1c–9] We have previously demonstrated that vacuum filtration of CCG dispersion, followed by drying, can lead to the formation of ultrastrong graphene papers in which individual sheets are stacked in a nearly parallel fashion.[9a] However, because substantial restacking occurs in such an oriented structure,[9a] as-prepared graphene-paper-based supercapacitors only display a moderate performance.[10]

Our reexamination of the formation mechanism of the graphene paper has revealed that serious restacking does not occur in the filtration process. When the filtration is just completed (no CCG dispersion is left on the filter), the resultant film is found to remain wet. As-formed wet film, without any drying, can be peeled off from the filter membrane directly (Figure 1a). The wet film is found to contain ≈92 wt% water. Despite being highly swollen by water, the SSG film is still very conductive. An SSG film containing 0.045 mg cm^{-2} of CCG gives a sheet resistivity of 1860 Ω $square^{-1}$ (whilst its corresponding freeze-dried film is 740 Ω $square^{-1}$) and the high conductivity suggests that the CCG sheets in the SSG film are well connected with each other.

If the SSG film is subjected to freeze-drying, little shrinkage is observed in the lateral dimension but its thickness is reduced to ≈4.6% of its wet thickness. Scanning electron microscopy (SEM) analysis of the freeze-dried sample (Figure 1d) reveals a layered but wrinkled structure. This layering or self-orientation phenomenon was also previously observed in graphene paper prepared by vacuum filtration.[1c–9] In contrast to the dried samples, the SSG film gives no detectable X-ray diffraction (XRD) peak at 22.7°. A diffraction peak appears at this angle for the dried films, corresponding to a *d*-spacing of 0.39 nm.[9a] (Figure 1e). This result, in conjunction with the observation of the drastic shrinkage upon freeze drying, indicates that despite being arranged in a nearly parallel manner, the graphene sheets in the SSG film remain largely separated by water.

The finding that CCG sheets are largely kept apart in the SSG film appears to be contradictory to the common expectation that the face-to-face arranged CCG sheets would collapse and restack to graphite as a result of their intersheet van der Waals attractions, as observed in the dried graphene paper[9a] and theoretical simulation.[11] We propose that a combination of the intrinsic corrugation and the colloidal interaction between CCG sheets has enabled the formation of such an unusual assembly. The key to this is recent experimental findings and theoretical simulations[12] that have suggested that freely suspended graphene sheets are not perfectly flat. To maintain their 2D structural stability at a finite temperature, free-standing graphene sheets must be corrugated to some extent, usually on the nanometer scale.[12a,b] In addition, recent studies have revealed that a portion of the carbon atoms in the CCG sheets are sp^3-hybridized and topological defects are present in the CCG sheets.[13] These defects would inevitably cause additional distortion to the flatness. Corrugation was also commonly observed in the dried powders of CCG[3a,4] as well as in its polymer nanocomposites.[14] On the basis of these observations, we speculate that the CCG sheets dispersed in solution must also be microscopically corrugated. When corrugated CCG sheets are stacked together on the filter membrane, the intersheet contact area is limited due to this corrugation and as a consequence of its high molecular stiffness. In particular, carboxylic acid groups are known to exist in CCG[4–7] and when the hydrated CCG sheets adhere together during filtration, the intersheet electrostatic repulsions caused by these negatively charged groups become more prominent, preventing them from complete stacking. Additionally, due to the presence of hydrophilic groups on the surface, water can be absorbed on the CCG surface quite tightly to induce repulsive hydration forces between sheets. It is known that hydration forces, which prevail in biological liquids, cellular membranes, and many other processes, are strong short-range, repulsive forces that increase exponentially with the distance of colloidal particles.[8] The formation of this special graphene/water hybrid structure is therefore a result of an elaborate balance of these repulsive interactions and the intersheet π–π attractions.

It is noteworthy that like many biological tissues, the oriented SSG film is a metastable material. If dried, the structure is not recoverable. Once the water is removed by drying, the π–π attractions become dominant and can cause partial flattening and better stacking of graphene sheets as evident in the XRD analysis. This flattening further enhances the intersheet π–π attractions, making it difficult for the dried CCG film to re-swell in water. As will be discussed further, the trapped water in the film is an integral part of the graphene assembly and is vital for the stacked graphene sheets to achieve exceptional performance. It is the presence of the water that activates the colloidal interaction between sheets, enabling retention of the highly open pore structure of the resulting film.

It is known that the performance of carbon materials as electrodes for supercapacitors is highly dependent on both the accessible specific surface area and pore structure.[15] To examine the pore structure and the surface accessibility of graphene sheets in the SSG film and its potential application as electrodes for energy storage devices, we studied the electrochemical properties of SSG-based supercapacitors in a traditional two-electrode, "sandwich" configuration. Electrochemical

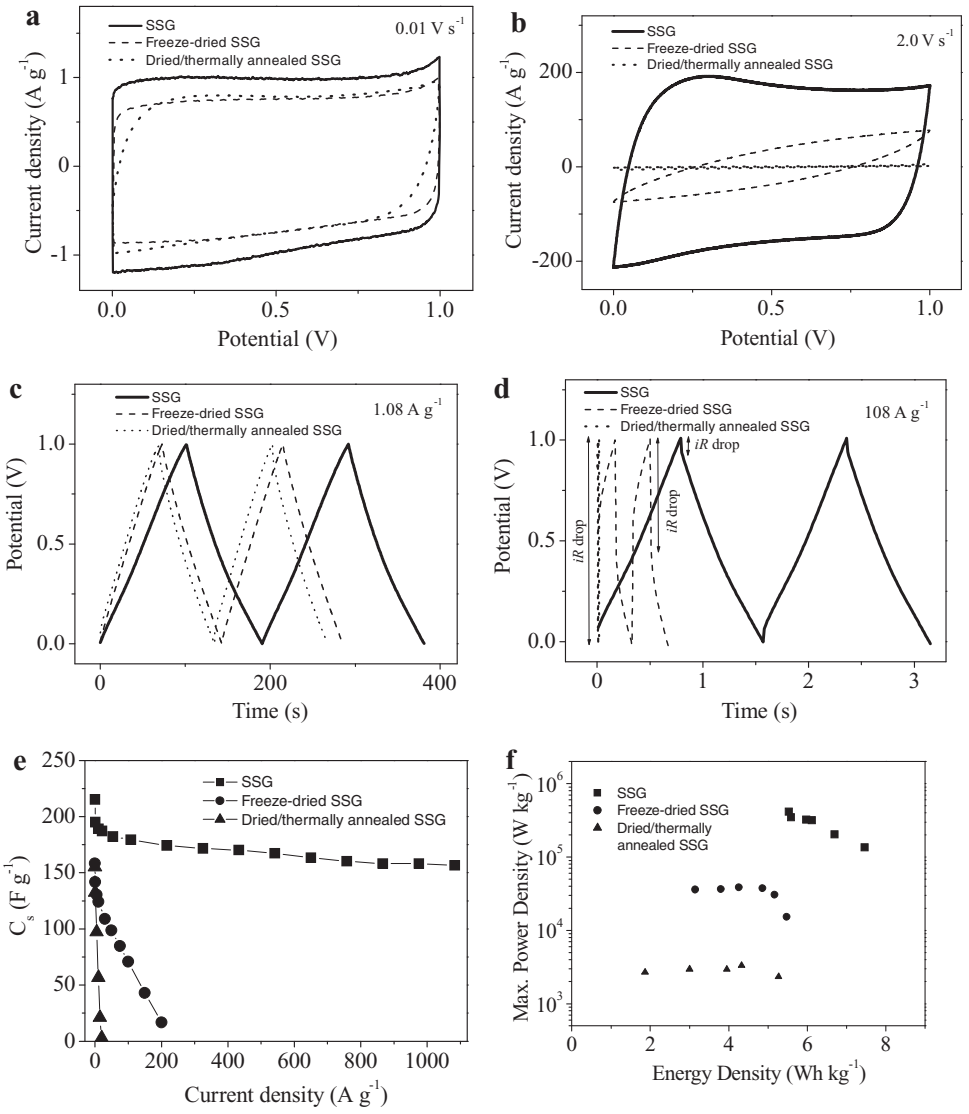

Figure 2. Electrochemical characterization of the SSG film-based supercapacitors (red curves). a,b) CV curves obtained at slow (a) and fast (b) scan rates, obtained using a VMP2/Z multichannel potentiostat. c,d) Charge/discharge curves obtained at different current densities. e) Gravimetric capacitances measured at various charge/discharge currents. f) Ragone plots of the SSG films-based supercapacitors. The energy density and maximum peak power density are against the mass of the active materials (CCG) in the electrodes. The freeze-dried samples were also tested for comparison. All the tests with a 1 V operation voltage were carried out in 1.0 M aqueous H_2SO_4 electrolyte.

characterization (**Figure 2**) reveals that the SSG film-based supercapacitor displays superior performance without the need for any other binders or electroactive additives. The SSG film containing 0.45 mg cm^{-2} of CCG gives a specific capacitance of up to 215.0 F g^{-1} in an aqueous electrolyte. More significantly, compared to other carbon materials, including delicately engineered activated carbon containing large mesopores[15d] and carbon nanotube films,[16] the specific capacitance of the SSG film is all much less affected by the charge/discharge rates (Figure 2e). The cyclic voltammetry (CV) profile still retains a rectangular shape at an ultrafast scan rate of ≈2.0 to 10.0 V s^{-1} (Figure 2b and Figure S1e, Supporting Information). A capacitance of 156.5 F g^{-1} can be obtained even when the supercapacitor is operated at an ultrafast charge/discharge rate of 1080 A g^{-1}. This means that the supercapacitors can be charged/discharged at the millisecond scale (Figure S1, Supporting Information). The SSG film can provide a maximum power density of 414.0 kW kg^{-1} at a discharge current of 108 A g^{-1}, 1 to 3 orders of magnitude higher than freeze-dried/thermally annealed counterparts and other carbon materials.[15b] Additionally, the SSG film exhibits excellent cyclability. It can retain over 97% of capacitance over 10 000 cycles even under a high operation current of 100 A g^{-1} (Figure S1, Supporting Information).

To ascertain the origin of the exceptional performance of the SSG-based supercapacitor, we also tested the electrochemical performance of the dried SSG films for comparison. As with other carbon materials,[15b] the capacitances of the dried SSG films drop substantially when the operation current is increased (Figure 2c–e). The thermally annealed film shows almost no capacitance when the loading current exceeds 20 A g^{-1}. Given

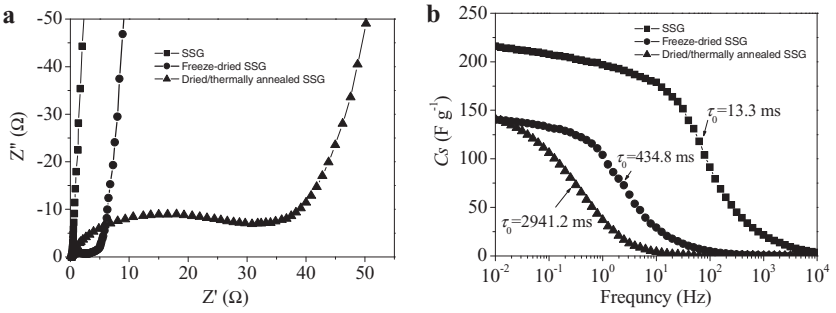

Figure 3. Frequency response of the SSG film-based supercapacitors 1.0 M aqueous H_2SO_4 electrolyte. a) Nyquist plots and b) Bode plots of the frequency response of the capacitance. The results for the freeze-dried samples are shown for comparison.

that the chemical structure of both the wet and dried CCG films is identical, the superior performance of the SSG film can only be ascribed to the formation of a highly open, continuous pore structure across the entire film through the ordered assembly. The SSG film undergoes a drastic restacking and shrinkage in volume (by a factor of ≈20) upon drying and thermally annealing resulting in a significant reduction in surface area and particularly pore volume. The pore size in the SSG film should therefore be much larger and the diffusion of ions is much facilitated. Note that the performance of the freeze-dried sample is indeed comparable to that of many porous carbon materials reported in the literature that perform well. By comparing the data collected from the SSG film with those of the dried samples shown in Figure 2 and **Figure 3**, one can gain a rough idea about how significantly the SSG film outperforms other porous carbon materials.

The fast ion diffusion in the SSG film is further confirmed by the Nyquist plots (Figure 3a). The projected length of the Warburg-type line (the slope of the 45° portion of the curve) on the real axis characterizes the ion diffusion process from solution into the intersheet region of the graphene films. The Warburg-type line of the SSG-based supercapacitor is the shortest, suggesting the fastest ion diffusion in the SSG film. The high-frequency intercept along the *x*-axis in the Nyquist plot corresponds to the internal resistance of the supercapacitors, which determines the operation rate of a capacitor (power capability). As shown in Figure 3a, the internal resistance of SSG is much less than that of the dried ones. Bode plots of the frequency response of capacitance (Figure 3b) also reveal the significant influence of the hydration state on the rate of ion transport. The operating frequency (the frequency at which the capacitance is 50% of its maximum value)[17] of SSG, dried SSG, and dried/annealed samples are 75, 2.3, and 0.34 Hz, respectively, corresponding to the characteristic relaxation time constants τ_0 = 13.3, 434.8, and 2941.2 ms, showing a difference in the frequency response of more than 200 times. The operating frequency of the SSG film (75 Hz) is higher than that of the microporous carbon with the pores well aligned (≈10 Hz)[17] and onion-like carbon (≈38 Hz) in a microsized device configuration.[18] These experiments clearly indicate the importance of water and the colloidal interaction in the formation and retention of such a unique pore structure. To our knowledge, no other porous carbon nanomaterials can offer a capacitance as high as the SSG film in a traditional macrosized device at such high operation rates (see a recent review for the state of the art of the carbon-based supercapacitors).[6]

Although we have only demonstrated the performance of the SSG film in aqueous electrolytes, the water in the film can be easily exchanged with other solvents. We have exchanged the water with a typical room-temperature ionic liquid (IL), 1-ethyl-3-methylimidazolium tetrafluoroborate, by vacuum evaporation of water in the presence of the IL. The operation voltage for the SSG-based supercapacitor can thus be increased to 4 V (vs 1 V in aqueous electrolyte). At room temperature, the IL-exchanged SSG film-based supercapacitor can offer a specific capacitance of up to 273.1 F g^{-1} and an energy density and maximum power density up to 150.9 Wh kg^{-1} and 776.8 kW kg^{-1}, respectively (**Figure 4**). Note that the highest energy density is comparable to that of lithium ion batteries (≈150 Wh kg^{-1}, against the mass of the active materials in the electrodes).[19] Both the energy density and average power density (Figure S2, Supporting Information) of the IL-exchanged SSG film are also significantly higher than those of highly curved yet dried graphene films.[2k] The operation rate is also much broader than that of the dried ones.[2k] These results again demonstrate the dramatic effect of solvation on the prevention of the restacking/aggregation of graphene sheets.

Porous carbon films have long been sought after and extensively studied for a variety of applications such as electrodes of various energy storage and conversion devices, catalyst supports, and chemical-resistant separation membranes.[15b–20] The traditional strategies for the synthesis of porous carbon generally involve high-temperature carbonization of organic precursors, carbides, and more recently graphene oxide.[2g–21] The pore structure is usually formed and retained solely through the cross-linking of hard carbon units. As the synthesis involves high-temperature treatment, serious aggregation or restacking occurs inevitably. Note that previous efforts to make graphene-based porous carbon film have predominantly involved drying and/or thermally annealing of the products including the highly curved graphene recently reported.[2k] As demonstrated here, these routine operations can result in limited performance of the resultant supercapacitors.[2a–f,h–j] In contrast, our strategy is based on low-temperature, liquid-phase, and bottom-up assembly of pre-synthesized graphene sheets in an ordered fashion. As described above, the synthesis is performed in solution so the principles of colloidal chemistry can be adopted to control both the assembly process and the pore structure. It is this soft assembly process makes it possible to form an oriented yet well-separated graphene assembly.

As for restacking control, a straightforward way that has been reported in the literature is to intercalate other hard species, such as polymers, nanoparticles, and even carbon nanotubes, between graphene sheets.[6a] Compared to the intercalation route, our soft strategy is superior in terms of simplicity, effectiveness, and processing and materials cost. As we recently demonstrated, the insertion of carbon nanotubes into the CCG sheets can significantly improve their electrochemical

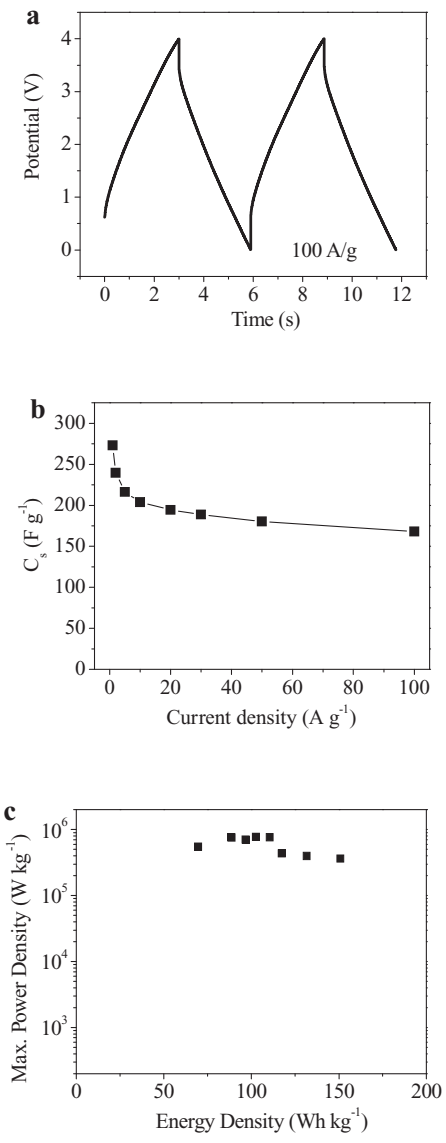

Figure 4. Electrochemical characterization of supercapacitors based on $EMIMBF_4$-exchanged SSG films with $EMIMBF_4$ as electrolyte. The water in SSG film was exchanged with the ionic liquid under vacuum at 100 °C. a) Typical charge/discharge curves at the current density of 100 A g^{-1}. b) Gravimetric capacitances measured at various charge/discharge current densities. c) Ragone plots (energy density vs maximum peak power density).

performance.[10] Nevertheless, the power density of the resulting supercapacitor is still not as impressive as that of the SSG films. Given the extraordinary supercapacitor performance and ease of cost-effective and scalable synthesis of such graphene films, our discovery is thus expected to greatly boost the development of the next generation of ultrafast energy storage devices, not only for consumer electronics, but also for other large-scale applications such as in electrical vehicles, for storage of renewable energy (e.g., wind and solar energy), and for smart electricity grid.

In summary, aggregation and restacking are a major hurdle that limits individual graphene sheets from realizing their full potential in an assembled bulk form. By taking advantage of the intrinsic corrugation and the colloidal interaction between chemically converted graphene sheets, we have demonstrated that face-to-face-stacked multilayered graphene sheets can remain largely separated in a solvated state, providing an amazingly simple strategy for addressing the key challenge that has limited the large-scale application of graphene. The resultant robust multilayered graphene film can provide a highly open pore structure, allowing the electrolyte solution to easily access to the surface of individual sheets. This has made it possible to combine ultrahigh power density and high energy density in graphene-based supercapacitors and to allow the device operational at high rates. Apart from its great potential as a new generation of nanostructured electrodes for ultrafast and high-capacitance energy storage devices, we expect that this unique macroscopic graphene assembly is also very promising for a broad range of other technological applications including electrodes for electrochemical sensors and actuators, water purification, and biomedical devices. The SSG film also has the potential to be a unique experimental platform for future research on the electronic properties of graphene assemblies, nanofiltration, and pseudo-2D nanofluidics. We expect that the success in addressing the restacking problem of graphene using this simple, bioinspired strategy will open up numerous opportunities for the application of graphene in a bulk form.

Experimental Section

Fabrication of the Solvated Graphene (SSG) Film: The chemically converted graphene (CCG) dispersion was prepared by chemical reduction of a graphene oxide (GO) solution that was obtained by chemical oxidation and exfoliation of natural graphite. The details of the synthetic procedure and structural characterization have been reported in a previous publication.[7] The lateral size of the obtained CCG sheets ranged from a few hundred nanometers to 1 μm. To prepare the SSG film, a certain amount of CCG dispersion was filtered through a mixed cellulose ester filter membrane (0.05-μm pore size, Millipore) by vacuum suction. Once the filtration was completed, the resultant SSG film was immediately transferred to a Petri dish and immersed in water overnight to remove the remaining ammonia and unreacted hydrazine. Relative thick films were carefully peeled off from the filter membrane using tweezers and were used for various measurements. All SSG films were stored in water prior to use. The films were cut into required sizes for various tests using scissors. The content of CCG in the SSG films was determined by weighing a whole piece of film (9.6 cm^2) dried at 100 °C for 12 h. The weight of the films was pre-estimated by the actual area of the films. The weight was then checked again after testing (after removing the electrolytes by dialysis and drying). If there was any inconsistency (usually smaller than 1.5%), the value obtained by direct weighing of the tested sample was used.

Structural and Properties Characterization: The XRD patterns were recorded on a Philips 1130 X-ray diffractometer (40 kV, 25 mA, Cu Kα radiation, λ = 1.5418 Å) at room temperature. The data were collected from 2° to 70° with the scan rate of 2° min^{-1} and steps of 0.02°. SEM images were obtained using a JEOL JSM 7001F scanning electron microscope.

Electrochemical Testing: Prototype supercapacitors using the graphene films as electrodes were assembled in a symmetrical two-electrode configuration using a similar procedure to that reported by Hu et al.[16] Before assembly, the SSG films were exchanged with the electrolyte solution for 3 h. To make the supercapacitor, two pieces of graphene films of the same size (≈1 cm by 1 cm) were first attached on two Pt foils. At the end of the Pt foil, a platinum wire was clipped onto the foil

by a toothless alligator clip, which was then connected to a Versastat-4 or VMP2/Z multichannel potentiostat/galvanostat (Princeton Applied Research) for electrochemical characterization. The overlapping parts were assembled with a filter paper sandwiched in between. The supercapacitors were wrapped with parafilm and then infiltrated with H_2SO_4 (1.0 M) as the electrolyte solution. The galvanostatic charge/discharge tests were carried out between 0 and 1 V at current densities between 0.1 and 1080 A g^{-1}. Unless specifically stated in the figure captions, the electrochemical data were obtained on the Versastat-4 potentiostat. The details for calculation of capacitance and power density are provided in the Supporting Information.

Supporting Information

Supporting Information is available from the Wiley Online Library or from the author.

Acknowledgements

X.Y., J.Z., and L.Q. contributed equally to this work. The authors acknowledge the financial support from the Australian Research Council. X.Y. is a visiting PhD student from Shanghai Jiao Tong University. J.Z. is a visiting fellow from Nanjing University of Science and Technology supported by the China Scholarship Council. This work made use of the facilities at the Monash Centre for Electron Microscopy. The authors thank G. P. Simon for proofreading and very helpful discussions with this manuscript.

Received: January 21, 2011
Published online: May 10, 2011

[1] a) A. K. Geim, *Science* **2009**, *324*, 1530; b) S. Park, R. S. Ruoff, *Nat. Nanotechnol.* **2009**, *4*, 217; c) D. A. Dikin, S. Stankovich, E. J. Zimney, R. D. Piner, G. H. B. Dommett, G. Evmenenko, S. T. Nguyen, R. S. Ruoff, *Nature* **2007**, *448*, 457; d) M. Segal, *Nat. Nanotechnol.* **2009**, *4*, 611; e) X. L. Li, G. Y. Zhang, X. D. Bai, X. M. Sun, X. R. Wang, E. Wang, H. J. Dai, *Nat. Nanotechnol.* **2008**, *3*, 538; f) D. Li, R. B. Kaner, *Science* **2008**, *320*, 1170.

[2] See examples: a) M. D. Stoller, S. J. Park, Y. W. Zhu, J. H. An, R. S. Ruoff, *Nano Lett.* **2008**, *8*, 3498; b) S. R. C. Vivekchand, C. S. Rout, K. S. Subrahmanyam, A. Govindaraj, C. N. R. Rao, *J. Chem. Sci.* **2008**, *120*, 9; c) D. W. Wang, F. Li, J. P. Zhao, W. C. Ren, Z. G. Chen, J. Tan, Z. S. Wu, I. Gentle, G. Q. Lu, H. M. Cheng, *ACS Nano* **2009**, *3*, 1745; d) H. L. Wang, H. S. Casalongue, Y. Y. Liang, H. J. Dai, *J. Am. Chem. Soc.* **2010**, *132*, 7472; e) Y. Wang, Z. Q. Shi, Y. Huang, Y. F. Ma, C. Y. Wang, M. M. Chen, Y. S. Chen, *J. Phys. Chem. C* **2009**, *113*, 13103; f) Q. Wu, Y. X. Xu, Z. Y. Yao, A. R. Liu, G. Q. Shi, *ACS Nano* **2010**, *4*, 1963; g) Y. X. Xu, K. X. Sheng, C. Li, G. Q. Shi, *ACS Nano* **2010**, *4*, 4324; h) D. S. Yu, L. M. Dai, *J. Phys. Chem. Lett.* **2010**, *1*, 467; i) L. L. Zhang, R. Zhou, X. S. Zhao, *J. Mater. Chem.* **2010**, *20*, 5983; j) Y. W. Zhu, S. Murali, M. D. Stoller, A. Velamakanni, R. D. Piner, R. S. Ruoff, *Carbon* **2010**, *48*, 2118; k) C. Liu, Z. Yu, D. Neff, A. Zhamu, B. Z. Jang, *Nano Lett.* **2010**, *10*, 4863.

[3] a) H. C. Schniepp, J. L. Li, M. J. McAllister, H. Sai, M. Herrera-Alonso, D. H. Adamson, R. K. Prud'homme, R. Car, D. A. Saville, I. A. Aksay, *J. Phys. Chem. B* **2006**, *110*, 8535; b) N. Behabtu, J. R. Lomeda, M. J. Green, A. L. Higginbotham, A. Sinitskii, D. V. Kosynkin, D. Tsentalovich, A. N. G. Parra-Vasquez, J. Schmidt, E. Kesselman, Y. Cohen, Y. Talmon, J. M. Tour, M. Pasquali, *Nat. Nanotechnol.* **2010**, *5*, 406; c) Y. Hernandez, V. Nicolosi, M. Lotya, F. M. Blighe, Z. Y. Sun, S. De, I. T. McGovern, B. Holland, M. Byrne, Y. K. Gun'ko, J. J. Boland, P. Niraj, G. Duesberg, S. Krishnamurthy, R. Goodhue, J. Hutchison, V. Scardaci, A. C. Ferrari, J. N. Coleman, *Nat. Nanotechnol.* **2008**, *3*, 563.

[4] S. Stankovich, D. A. Dikin, R. D. Piner, K. A. Kohlhaas, A. Kleinhammes, Y. Jia, Y. Wu, S. T. Nguyen, R. S. Ruoff, *Carbon* **2007**, *45*, 1558.

[5] J. R. Miller, R. A. Outlaw, B. C. Holloway, *Science* **2010**, *329*, 1637.

[6] a) D. S. Su, R. Schlogl, *ChemSuschem* **2010**, *3*, 136; b) C. Liu, F. Li, L. P. Ma, H. M. Cheng, *Adv. Mater.* **2010**, *22*, E28.

[7] D. Li, M. B. Muller, S. Gilje, R. B. Kaner, G. G. Wallace, *Nat. Nanotechnol.* **2008**, *3*, 101.

[8] Y. Liang, N. Hilal, P. Langston, V. Starov, *Adv. Colloid Interface Sci.* **2007**, *134–135*, 151.

[9] a) H. Chen, M. B. Muller, K. J. Gilmore, G. G. Wallace, D. Li, *Adv. Mater.* **2008**, *20*, 3557; b) Y. X. Xu, H. Bai, G. W. Lu, C. Li, G. Q. Shi, *J. Am. Chem. Soc.* **2008**, *130*, 5856; c) S. Park, J. H. An, R. D. Piner, I. Jung, D. X. Yang, A. Velamakanni, S. T. Nguyen, R. S. Ruoff, *Chem. Mater.* **2008**, *20*, 6592.

[10] L. Qiu, X. Yang, X. Gou, W. Yang, Z. F. Ma, G. G. Wallace, D. Li, *Chem Eur. J.* **2010**, *16*, 10653.

[11] C. J. Shih, S. C. Lin, M. S. Strano, D. Blankschtein, *J. Am. Chem. Soc.* **2010**, *132*, 14638.

[12] a) J. C. Meyer, A. K. Geim, M. I. Katsnelson, K. S. Novoselov, T. J. Booth, S. Roth, *Nature* **2007**, *446*, 60; b) A. Fasolino, J. H. Los, M. I. Katsnelson, *Nat. Mater.* **2007**, *6*, 858; c) J. M. Carlsson, *Nat. Mater.* **2007**, *6*, 801.

[13] C. Gomez-Navarro, J. C. Meyer, R. S. Sundaram, A. Chuvilin, S. Kurasch, M. Burghard, K. Kern, U. Kaiser, *Nano Lett.* **2010**, *10*, 1144.

[14] S. Stankovich, D. A. Dikin, G. H. B. Dommett, K. M. Kohlhaas, E. J. Zimney, E. A. Stach, R. D. Piner, S. T. Nguyen, R. S. Ruoff, *Nature* **2006**, *442*, 282.

[15] a) B. E. Conway, *Electrochemical Supercapacitors* Vol. 1, Kluwer Academic/Plenum Publishers, New York **1999**; b) A. G. Pandolfo, A. F. Hollenkamp, *J. Power Sources* **2006**, *157*, 11; c) J. Chmiola, G. Yushin, Y. Gogotsi, C. Portet, P. Simon, P. L. Taberna, *Science* **2006**, *313*, 1760; d) D. W. Wang, F. Li, M. Liu, G. Q. Lu, H. M. Cheng, *Angew. Chem. Int. Ed.* **2008**, *47*, 373.

[16] L. B. Hu, J. W. Choi, Y. Yang, S. Jeong, F. La Mantia, L. F. Cui, Y. Cui, *Proc. Natl. Acad. Sci. USA* **2009**, *106*, 21490.

[17] A. Kajdos, A. Kvit, F. Jones, J. Jagiello, G. Yushin, *J. Am. Chem. Soc.* **2010**, *132*, 3252.

[18] D. Pech, B. Magali, D. Hugo, H. Peihua, M. Vadym, G. Yury, T. Pierre-Louis, S. Patrice, *Nat. Nanotechnol.* **2010**, *5*, 651.

[19] a) M. R. Palacin, *Chem. Soc. Rev.* **2009**, *38*, 2565; b) S. W. Lee, N. Yabuuchi, B. M. Gallant, S. Chen, B. S. Kim, P. T. Hammond, Y. Shao-Horn, *Nat. Nanotechnol.* **2010**, *5*, 531.

[20] a) A. F. Ismail, L. I. B. David, *J. Membr. Sci.* **2001**, *193*, 1; b) J. Lee, J. Kim, T. Hyeon, *Adv. Mater.* **2006**, *18*, 2073.

[21] a) F. Liu, T. S. Seo, *Adv. Funct. Mater.* **2010**, *20*, 1930; b) M. A. Worsley, P. J. Pauzauskie, T. Y. Olson, J. Biener, J. H. Satcher, T. F. Baumann, *J. Am. Chem. Soc.* **2010**, *132*, 14067.